Appendix I. Air Dispersion Modeling

I-1. Modeling Approach

Given the objectives of this study and the availability of onsite meteorological data formatted for the Industrial Source Complex (ISC) model, two models were considered candidates for this study: the ISC model (EPA, 1995) and the CALPUFF model (Scire et al., 1995). ISC is a straight-line Gaussian plume model recommended in EPA's "User's Guide for the Industrial Source Complex (ISC3) Dispersion Models" Guideline on Air Quality Models" (EPA, 1995c) for use in simple terrain settings. CALPUFF is a Gaussian puff dispersion model that has been formulated to provide a more refined estimate of air quality impacts than ISC in areas of complex terrain and meteorology. CALPUFF is more accurate than the ISC model in areas of complex meteorology as over multiple hours of transport CALPUFF uses each hour of wind to develop a curved, as opposed to the ISC straight-line, transport. This hour-by-hour treatment of transport in CALPUFF results in a better estimate of where SSFL emissions are expected to have repeated high concentrations and areas with relatively insignificant concentration impacts are located.

I-2. Model Description

CALPUFF is a non-steady-state puff dispersion model that can simulate the effects of time- and space-varying meteorological conditions on pollutant transport, transformation, and removal. CALPUFF can use single-station hourly varying winds or hourly varying complex three-dimensional meteorological fields. CALPUFF accounts for vertical wind shear, over water transport, and coastal interaction effects. CALPUFF contains algorithms for near-source effects such as building downwash, transitional plume rise, partial plume penetration, and subgrid scale terrain interactions. CALPUFF contains algorithms for longer range effects such as chemical transformation and pollutant removal (wet scavenging and dry deposition).

CALPUFF uses a Gaussian dispersion treatment recommended in EPA modeling guidance for simple terrain settings. CALPUFF treats arbitrarily-varying point source and gridded area-source emissions. CALPUFF considers point sources (buoyant or otherwise), area sources, line sources, and volume sources. Locations are specified separately for each source. Pasquill-Gifford dispersion coefficients are used for rural applications, and McElroy-Pooler dispersion coefficients are applied in urban applications. Plume rise is calculated for point sources according to Briggs' formulas for buoyant or momentum-dominated sources.

In the CALPUFF model, receptors can be specified in an organized polar or rectangular grid or as discrete receptor locations. Meteorological data are input as hourly averages. Ambient concentrations are output for short-term (1-hour) periods and post-processing is performed to obtain long-term (annual or multi-annual) averages. Model input data for CALPUFF include source characteristics, meteorological data, and topographical data.

I-3. Receptors

The CALPUFF model requires input of receptor coordinates at which to predict ambient air impacts. To allow concentrations to be estimated for 50 kilometers in all directions from the

SSFL facility, receptors were specified for a grid of 101 (west to east) by 101 (south to north) points spaced at 1,000-meter intervals and centered over the SSFL facility. Figure 3-2 shows the area covered by these 10,201 receptors. The southwest corner receptor has a UTM Easting (UTM X) of 295000 m and a UTM Northing (UTM Y) of 3739000 m. These UTM coordinates are for UTM Zone 11 and for the North American Datum of 1983 (NAD83), which is an earth-centered datum based on the Geodetic Reference System of 1980.

Figure I-1a. Area Covered by the CALPUFF Receptors

Note: There are 10,201 receptors in the area, spaced at 1,000-meter intervals.

To provide better near field spatial coverage, **Figure I-1b** depicts an additional set of receptors spaced about 100-m a part that were developed and located along the SSFL property line.

Figure I-1b. Near field receptor coverage for CALPUFF modeling. The 138 near field receptors are along the SSFL property boundary and spaced about 100-m apart.

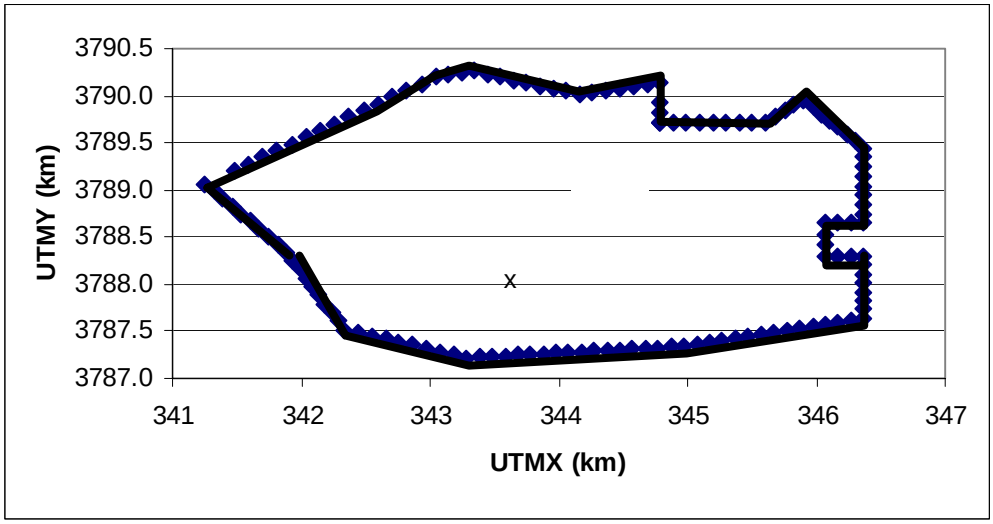

I-4. Model Options

The CALPUFF model was set to perform elevated terrain modeling; that is, receptors were assigned elevations other than the base elevation for the facility. Building downwash is a complex technical subject that has important ramifications in the field of air quality dispersion modeling. Essentially, as wind blows over building structures, a wake effect is created that can extend out to a distance of five times the minimum of the building height or perpendicular building width. This wake effect can influence the vertical extent to which stack emissions rise into the atmosphere.

I-5. Topographic Data

The National Cartographic Information Center (NCIC) distributes several types of digital elevation data sets produced by the U.S. Geographical Survey. These digital cartographic data consist of Digital Elevation Models (DEM), which are digital records of terrain elevations for ground positions at regularly spaced horizontal intervals produced as part of the National Mapping Program. Two distinct digital elevation data sets are available from the NCIC. The is the 1-degree DEM, a 1-by-1-degree block that provides the same coverage as half of a standard 1:250,000 scale map. Two 1-degree blocks are required to cover the entire area of a 1:250,000 series map. The second data set is the 7.5-minute DEM, which provides the same coverage as a 1:24,000 scale map. The 1-degree DEM data were used in this study.

The 1-degree DEM is produced by the Defense Mapping Agency and distributed by the NCIC. These data sets are available for most areas of the United States. The data format consists of elevations spaced at regular intervals of three arc-seconds and referenced by the geographic coordinate system (latitude/longitude). Three arc-seconds represent approximately 79 meters at 32 degrees latitude, the approximate latitude of the site. The 1-degree DEM data were analyzed to determine the elevation of receptors for this study.

I-6. Meteorological Data

I-6.1 Overview

Preprocessed ISC-ready meteorological data files prepared by Trinity Consultants were provided by Boeing. The meteorological data period begins January 1, 1994, and extends through December 31, 1997 (see Section 3.1.3). The files are based on surface meteorological data for 1994 through 1997, collected on-site at the SSFL in Area IV. The meteorological data include wind speed, wind direction, and temperature data. An upper-air data set was used principally to assign hourly mixing heights (rural and urban) within the ISC meteorological data files. The headers in the preprocessed files indicate that upper-air data from Miramar Naval Air Station (NKX) near San Diego were used. While the upper-air site at Los Angeles International Airport (LAX) is closer, LAX is located at the coast, while both SSFL and NKX are located on mesas inland from the coast and likely have similar mixing heights.

I-6.2 Long-Term Climatology

Climatological data from 1948 to 2003 were reviewed to determine whether the 1994–1997 meteorological data period used in this air quality analysis was representative of the longer time period during which SSFL operated. Precipitation measurements from a nearby site available from the Climate Diagnostic Center (CDC) reanalysis project were used in this analysis (http://www.cdc.noaa.gov/cdc/reanalysis).

The geopotential height at 500 mb and the temperature at 850 mb are used as indicators of stagnation. Periods with higher 500-mb height and higher 850-mb temperatures are often associated with lower wind speeds and less vertical mixing. Time series plots of monthly mean 850-mb heights and 850-mb temperatures for the years 1948 through 2003 were generated on the Climate Diagnostic Center's reanalysis project Web site for a 4 square degree area over southern California.

The time-series of monthly mean 500-mb geopotential heights is shown in Figure I-2, and the time series of monthly mean 850-mb temperatures appears in Figure I-3. In general, the years 1994 through 1997 appear to have experienced higher 500-mb heights and 850-mb temperatures than normal for the entire 1948–2003 period. However, none of the monthly mean values are extremes for the period. While the 1994–1997 period may have been slightly more stagnant than typical for the full historical period analyzed, it is reasonably representative of what occurred meteorologically during historical operations at the SSFL.

The site with long-term annual precipitation totals nearest the SSFL station is located at Canoga Park, California, which is about 15 kilometers southeast of the SSFL. Given its proximity to SSFL, there is good reason to believe that precipitation measurements recorded in Canoga Park can be relied upon to describe the associated historical pattern of precipitation at SSFL. In Section 3's Figure 3-8, which depicts the annual rainfall totals recorded by year at Canoga Park from 1948 to 2002, large squares identify rainfall totals for 1994 to 1997, and smaller diamonds identify rainfall totals in other years from 1949 to 2002.

The annual average rainfall from 1949 to 2002 was 16.2 inches, only 10 percent less than the annual average rainfall of 17.9 inches from 1994 to 1997. The standard deviation of the annual average rainfall from 1949 to 2002 was 9.1 inches, only 13 percent greater than the standard deviation of the annual average rainfall of 8.0 inches from 1994 to 1997. Since the Canoga Park rainfall statistics (annual average and standard deviation) for the longer-term time period of interest (1948-2002) and the 1994–1997 meteorological time period are similar, the meteorological data relied on in this air quality analysis (from 1994 to 1997) appear likely to be representative of the longer-term period of interest. It is also noted that review of climatological data suggests that the meteorological data for 1994 through 1997 are reasonably representative of the period of historical operations at the SSFL. The 500-mb height and 850-mb temperature data suggest that conditions in that period may have been more stagnant than typical. Therefore, the modeling results may be slightly conservative.

Figure I-2. Monthly Mean 500-mb Geopotential Heights for 1948–2003 over Southern California

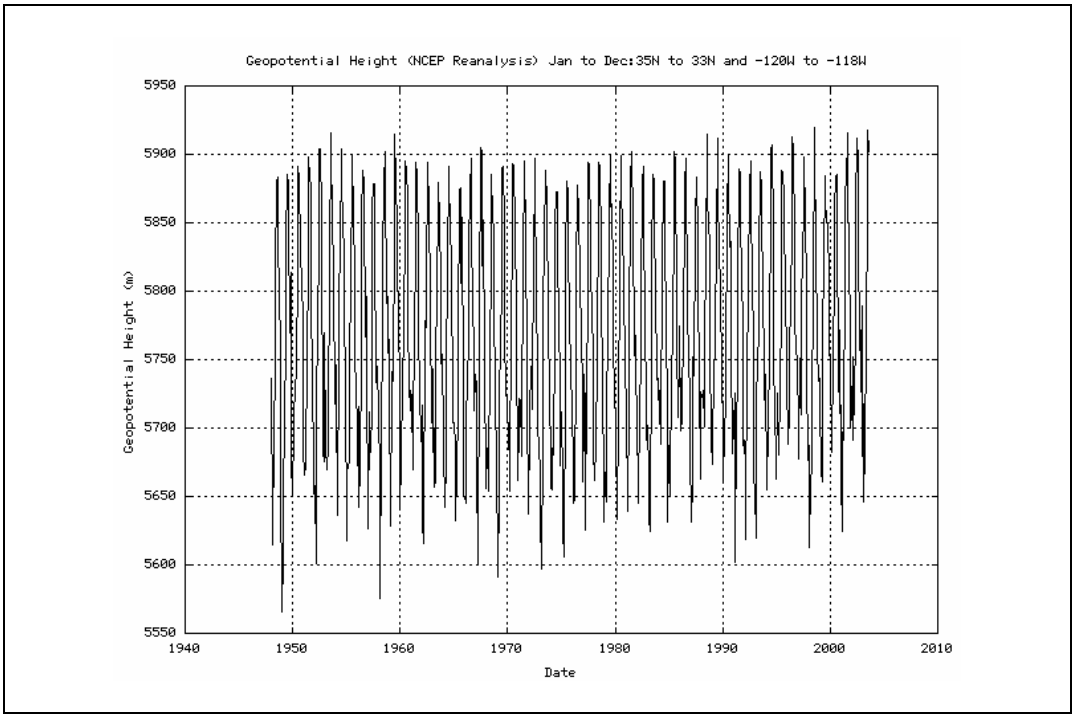

Figure I-3. Monthly Mean 850-mb Temperatures for 1948–2003 over Southern California

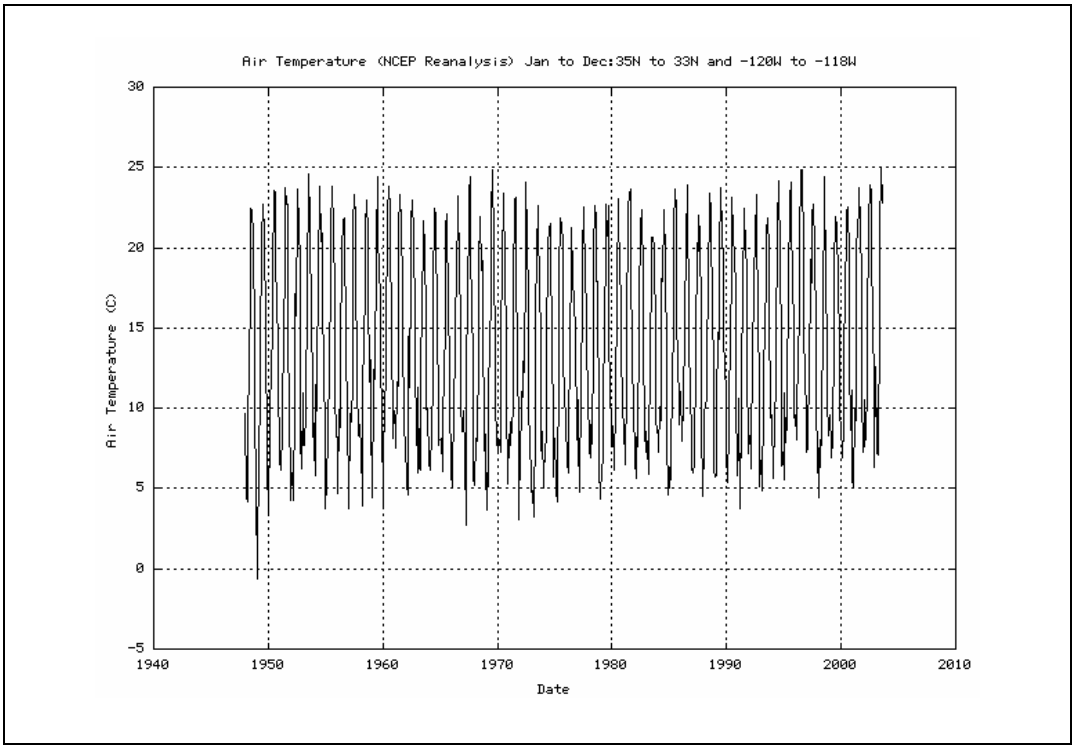

I-6.3 On-Site Wind Data Differences

During a number of site visits to SSFL the study team members personally observed wind directions in Areas II and III that were generally consistent with those in Area IV. In addition, winds observed during one site visit in a portion of Area I varied from those observed in Areas II, III and IV. Comparison of the available Area I and Area IV wind data revealed that the Area I site wind directions are at times rotated about 22 degrees counterclockwise from those recorded in Area IV, which is consistent with directional differences in the slope of the terrain at each location. It is believed that the terrain ridge west of Area I is a cause of this wind direction difference. This difference in Area I and Area IV wind direction is believed to have occurred during hours dominated by upslope and downslope flows. Upslope and downslope flows dominate when a weak synoptic weather pattern is present. A symptom of a weak synoptic weather pattern is surface flows with low wind speeds. Because the surface winds at SSFL were less than 2 knots 25% of the time and less than 4 knots 45% of the time, this weak synoptic weather pattern leading to different wind directions in Area I compared with Area IV could have occurred at least 25%, and possibly as frequently as 45%, of the time at this site. This complex wind flow behavior was not considered in the modeling performed in this study. For this reason, when interpreting the modeling results presented, it is important to recognize that, when the above specific complex wind patterns exist, the concentration predictions from Area I emission sources may be about 22 degrees counterclockwise from those estimated due to the use of Area IV wind data.

I-7. Emissions Data

Between 1953 and 1961, over 8,000 tests on rocket engines were completed. During the 1970s and 1980s, the site was primarily used to test engines for the NASA space shuttle program. The SSFL site is used today to build and test engines for the Atlas and Delta projects.

Emissions at the SSFL facility have occurred directly from RETs, the evaporation of solvents used to clean the rocket engines (i.e., TCE), the subsequent operation of STs to remove TCE from the groundwater, and the TTF. A review of historical emissions at the SSFL (Chapter 3) indicated that RETs were performed in dozens of locations, there were at least 10 locations with STs, and one location held the TTF. For modeling purposes these locations were consolidated into eight RET sources (modeled both as point and area sources), six ST sources, and one TTF source (see Appendix S for a complete air emission inventory). These 15 consolidated sources are summarized in Table 3-3 in Section 3.

Because the objective of this study was to model potential exposure patterns, a daily average emission rate of 1 g/s was used for each source. Using this “unit emission rate” facilitates combining predicted ambient air impacts from the individual emission source types and allows the calculation of cumulative impacts over multiple years.

Because terrain downwash is possible, RET emissions exit horizontally from the test stands, and stack information for the STs was not available, emissions from all sources were conservatively modeled for dispersion purposes with no plume rise. The source parameters used to model the release of emissions from all point and area sources are provided in Table I-1.

Table I-1. Parameters Used to Model the Release of Point and Area Source Emissions from the SSFL Facility

Point Source Parameters	Area Source Parameters
Stack height = 0 m agl	Area dimensions = 100 m x 100 m
Stack temperature = 273 degrees K	Effective height = 0 m
Stack diameter = 1 m	Base elevation = 0 m agl
Stack exit velocity = 0 m/s	Initial sigma-Z = 0 m

Documentation was not available regarding the time of day at which RETs occurred and the subsequent cleaning of rocket engines using chlorinated hydrocarbons. Based on anecdotal evidence and safety considerations, it is believed that testing occurred almost exclusively during daylight and dusk periods. It is also believed that, for safety reasons, almost all engine tests were conducted the same day the engines were prepared for testing. The implication is that the number of engine tests performed increased from morning to dusk. This is considered the "best estimate" for the diurnal profile of RET emissions for this study.

Due to the lack of documentation, the exact diurnal timing of emissions from RETs is unknown. As a sensitivity study, the ambient impact of RET emissions was also determined assuming that this activity took place uniformly throughout the day and night. Figure I-4 illustrates the effect of the "best estimate" rocket engine emissions increasing with time during the day compared to the uniform emission sensitivity study that was conducted.

TCE emissions from groundwater stripping towers were treated as occurring uniformly throughout each day, because there is no reason to believe the towers operated only during daylight hours. The timing of open burn activities is unknown, but it is assumed that they would have occurred almost exclusively during daylight hours for safety reasons. Therefore, the most representative temporal pattern would be to uniformly distribute open burning emissions during daylight hours. Table I-2 shows the three diurnal profiles used to model emissions from RET, ST, and TTF sources.

Figure I-4. Diurnal Variations in Emissions Used to Study the Impacts from RET Sources

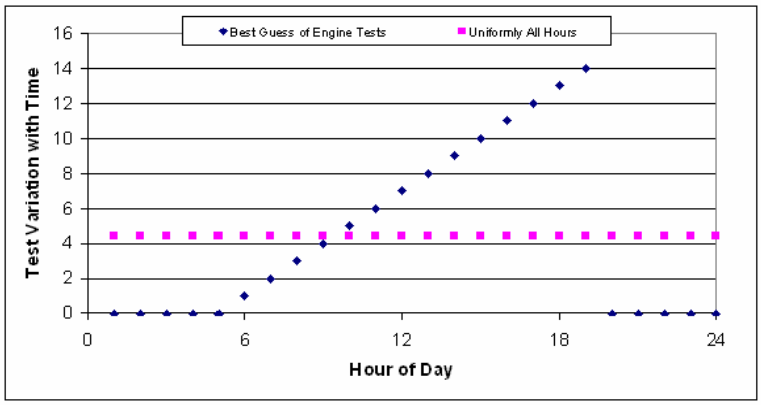

Table I-2. Diurnal Emission Profiles Used to Model and Study the Sensitivity of Ambient Impacts on the Timing of Emissions Released from the SSFL Facility.

Hour of the Day	Diurnal Emission Profile (g/s)		
	Daytime Increasing (Best Estimate for RET Sources)	Uniform (Best Estimate for ST Sources; Sensitivity for RET Sources)	Daytime Only (Best Estimate for TTF)
1	0	1.0	0
2	0	1.0	0
3	0	1.0	0
4	0	1.0	0
5	0	1.0	0
6	0	1.0	0
7	0.26	1.0	2.0
8	0.53	1.0	2.0
9	0.79	1.0	2.0
10	1.05	1.0	2.0
11	1.32	1.0	2.0
12	1.58	1.0	2.0
14	2.11	1.0	2.0
15	2.37	1.0	2.0
16	2.64	1.0	2.0
17	2.90	1.0	2.0
18	3.16	1.0	2.0
19	3.43	1.0	0
20	0	1.0	0
21	0	1.0	0
22	0	1.0	0
23	0	1.0	0
24	0	1.0	0

I-8. Model Application and Post-Processing

The CALPUFF model was run a total of 32 times for the RET locations. Each of the 8 RET stands was modeled as a point source and as an area using both the best-estimate diurnal profile and the uniform profile. Six simulations were carried out for the STs, one for each ST source using the uniform diurnal profile, and one for the TTF source using the daytime-only diurnal profile.

Each CALPUFF run generated four years (1987 to 1991) of hourly concentration predictions by receptor. For each receptor, these 4-years of hourly concentration predictions were averaged. The hourly averaging was done by the CALPUFF post-processor program (CALPOST). Adding together the multiplication of the emission rate by source type by the CALPUFF "unit emission rate" predicted ambient air concentration by source type and location resulted in the calculation of air toxic concentration averages over multiple years.

Because CALPUFF is a Gaussian dispersion model, it generated log-normally distributed ambient air concentrations that span roughly four orders of magnitude. Adjacent to the SSFL sources is the "hot spot" predicted by CALPUFF, where concentrations in ambient air are several

orders of magnitude greater than the rest of the 101-kilometer by 101-kilometer domain. To visually reflect this predicted behavior, CALPUFF predictions are presented using log-normal contours that increase in multiples of 10 (e.g., 10^{-3} µg/m^3, 10^{-2} µg/m^3, 10^{-1} µg/m^3, 1 µg/m^3, 10 µg/m^3). The CALDESK software program was used to overlay these contours on a map of SSFL and the surrounding area. Because CALDESK does not plot logarithmic contours, the CALPUFF concentrations were first converted to the logarithmic scale using Eq. I-1.

$$LC = \log_{10} (10^3 \times C) \qquad \text{(I-1)}$$

Where LC is the logarithmic concentration, which ranged from about 0 to 4 in this study, and C is the CALPUFF-generated multi-year average concentration in µg/m^3, which varies with receptor location. In the initial analysis of the model output, it was noted that concentrations decreased by three orders of magnitude within 5 kilometers of the SSFL boundary. Therefore, contour plots of logarithmic concentrations were prepared for a much smaller domain than actually modeled (Section 3.1.3).

I-9. Sensitivity Studies

I-9.1 Overview

In the present model simulations, atmospheric chemical degradation and dry and wet deposition processes were neglected since they were deemed to have a minor role in affecting the annual averaged concentrations. In order to assess the impact of the above model simplification a detailed sensitivity study was carried out. In these sensitivity studies the hourly maximum and 24-hour concentrations of species emitted from SSFL were calculated. However, instead of using a four-year hourly average, the four-year daily concentration distribution were examined to identify the range of possible hourly average and hourly maximum concentrations.

These sensitivity tests were based on an emission rate of 1 gram per second (1 g/s) daily average pollutant emission rate. Rocket engine testing was simulated as increasing in number from 6 a.m. to 7 p.m. The predicted concentrations were expressed in units of micrograms per cubic meter (µg/m^3). Hourly average concentrations denote an average of hourly concentrations obtained based on the four year of hourly meteorological data (1994-1997). The maximum hourly concentration is the highest one-hour concentration predicted from the four-years of hourly predictions.

I-9.1 Impact of Atmospheric Degradation

In order to assess the significance of atmospheric degradation reactions on the airborne concentrations of air toxics resulting from emissions from SSFL, a series of sensitivity analysis simulations were carried out. A chemical degradation process will affect the resulting airborne air toxic concentration if the reaction time scale is of the same order or much lower than the convective residence time (i.e., its travel time due to wind dispersion). Table I-3 lists the reaction lifetimes for SSFL emitted organic species of interest. Hydrazine and 1,3-butadiene have the shortest lifetime rates of reaction ranging from 0.5 hours to 6 hours. Of the other organic species, vinyl chloride has the next shortest reaction half-life of reaction ranging from 1.6 days to 3.9 days.

Table I-3. SSFL emitted organic species reported reactivity

Organic Species	Rocket Fuel	Reactivity (lifetime)	Reference
Hydrazine/UDMH/MMH	Hydrazine	≤ 5.3 hours	CARB (1997)
Benzene	Kerosene	12 days	CARB (2004a)
1,3-Butadiene		0.5 – 6 hours; formaldehyde is a produ	CARB (2004b)
Chloroform		150 to 230 days	CARB (1990b)
Vinylidene Chloride		1.3 days	CARB (2004c)
Methylene Chloride		80 to 250 days	CARB (1989)
Toluene		several days - summer several months - winte	WHO (2000)
Trichloroethylene		4 to 15 days	CARB (1990a)
Vinyl Chloride		1.6 to 3.9 days	CARB (1990d)
Xylene (Total)		14 to 25 hours	CARB (2004d)
TCA	-	5.4 years	CARB (2004e)

Atmospheric degradation of an emitted air toxic will decrease the emitted concentration of this species. The potential importance of including chemical reactions for hydrazine which has the shortest reaction half-life (5.3 hours) I illustrated in Figs. I-5 and I-6. For the population with the maximum concentration exposure shows a 1% decrease of the hourly average concentration and a 3% decrease in the hourly maximum concentrations when atmospheric degradation of hydrazine is included in the model simulation. For the hourly average and hourly maximum concentrations are two times lower with hydrazine chemistry than without. For the population least (minimum) impacted within 30 miles of the SSFL site, the hourly average and hourly maximum concentrations, calculated with hydrazine degradation included, were found to be ten and two times lower, respectively, relative to the case in which hydrazine degradation was neglected.

Figure I-5. Hourly average concentration statistics with and without hydrazine chemistry (i.e., atmospheric degradation). Note: Emission rate= 1g/s.

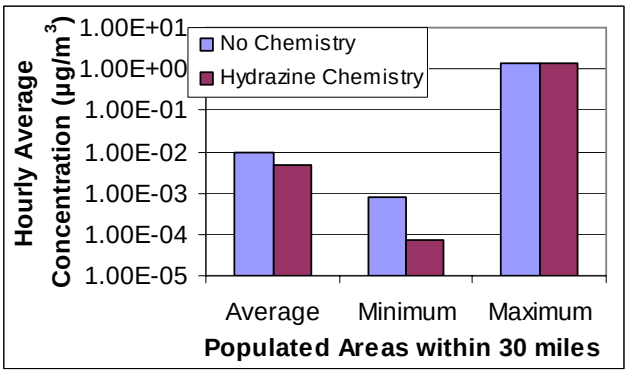

Figure I-6. Hourly maximum concentration statistics with and without hydrazine chemistry (i.e., atmospheric degradation). Note: Emission rate= 1g/s.

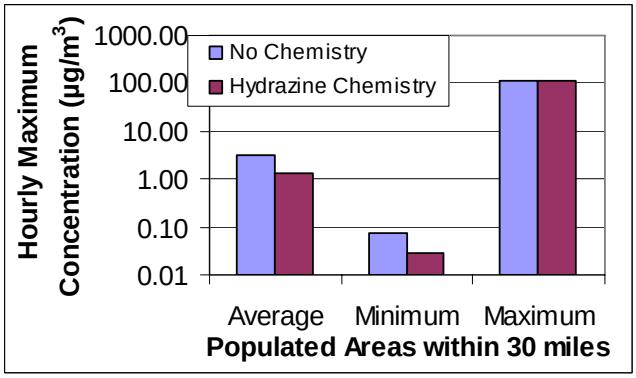

I-9.2 Impact of Dry Deposition

Dry deposition from the atmospheric onto the ground reduces the airborne concentration of toxic chemicals, particularly those that are in the particle-bound form. For example, heavy metals that were emitted from kerosene rocket fueled tests are likely to be present in the particulate form. Unfortunately, the PM_{10} size distribution (of most exposure concern) importance of particulate emissions from SSFL uncontrolled rocket engine tests is unknown. Therefore, the effect of dry deposition on heavy metal air concentrations was evaluated based on the U.S. Environmental Protection Agency (1998) reported PM_{10} size distribution (Table I-5) from distillate oil combustion (i.e., an uncontrolled industrial boiler.)

Table I-4. PM_{10} size distribution from uncontrolled industrial boiler burning distillate oil

Particle size (μm)	Cumulative mass less than or equal to stated size
10	100%
6	60%
2.5	24%
1.25	18%
1	16%
0.625	4%

Figures I-7 and I-8 compare predictions of air concentrations in populated areas from rocket engine test exhausts with and without dry deposition, using particle size distribution given in Table I-4. For the population with the maximum concentration exposure, there is a 0.5% to 0.8% decline in the hourly average and hourly maximum concentrations with dry deposition compared to the case without dry deposition. For the average population, the hourly average and hourly maximum concentrations are 30% and 15% lower, respectively, when dry deposition is considered. For the population least (minimum) impacted within 30 miles of the SSFL site, the hourly average and hourly maximum concentrations are 1.7 to 2.1 times lower, respectively, when dry deposition is considered relative to the case when dry deposition is neglected.

Figure I-7. Hourly average concentration statistics with and without dry deposition. Emission rate= 1 g/s.

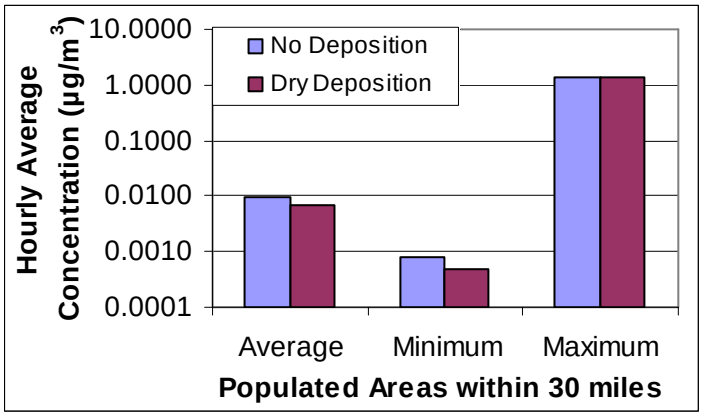

Figure I-8. Hourly maximum concentration statistics with and without dry deposition. Emission rate= 1 g/s.

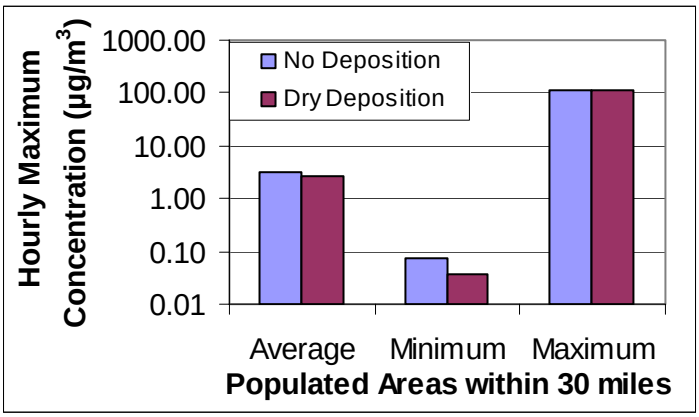

Figure I-9 summarizes predictions of dry deposition to the ground in populated areas from rocket engine test exhausts. The maximum dry deposition rate of 81,200 µg/m^2/yr is at the fenceline. The average and minimum dry deposition rates are 395 µg/m^2/yr and 29 µg/m^2/yr, respectively.

Figure I-9. Hourly average dry deposition statistics. Emission rate= 1 g/s.

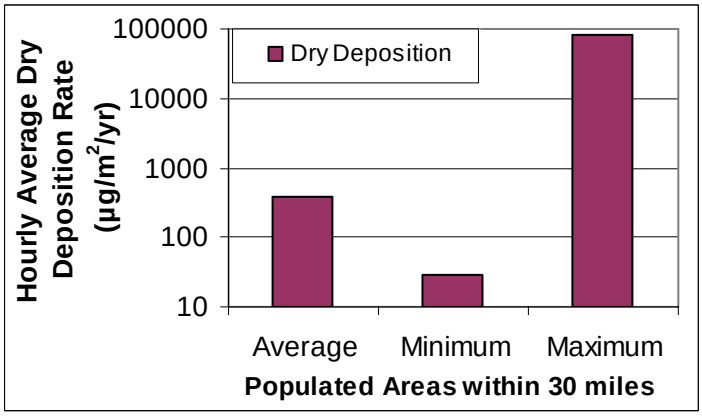

I-9.3 Impact of Wet Deposition

Although precipitation statistics for SSFL are somewhat different than for Los Angeles, precipitation statistics for Los Angeles should be reflective of the general trend at the SSFL, as Los Angeles is only about 30 miles southwest of the SSFL and at nearly the same elevation. Table I-5 summarizes mean monthly and annual number of hours with measurable precipitation at Los Angeles, California[I1]. Over the period of SSFL emissions, from 1950 through 1999 precipitation events in Los Angeles (Table I-5) spanned over less than 2.1 percent of the time. precipitation.

[I1] Source: The Western Regional Climate Center: http://www.wrcc.dri.edu/htmlfiles/hrsofppt.html

Table I-5. Mean monthly and mean annual number of hours with measurable precipitation at Los Angeles, California (http://www.wrcc.dri.edu/htmlfiles/hrsofppt.html).

	YEARS	JAN	FEB	MAR	APR	MAY	JUN	JUL	AUG	SEP	OCT	NOV	DEC	YEAR	% of HOURS
LOS ANGELES	1950-1999	41	35	30	15	4	1	1	1	4	5	19	26	181	2.1

There is the expectation that testing at the SSFL was conducted only during hours without precipitation. This would mean that wet deposition of chemicals emitted from SSFL would not be expected during a rocket engine test. Under even low winds, SSFL emissions would be transported 3.6 km from the test stand in an hour. Even if hours of wet deposition removed all air borne emissions released after 3.6 km, this would on average remove at most 2.1% of the chemicals released from the SSFL. The other 97.9% of emissions would remain airborne until exiting from the 30-km study (i.e., simulation) area or removed by atmospheric degradation and/or dry deposition. Given the above, it is clear that the absence of wet deposition in the present simulations would result in a conservative estimate of airborne concentrations. However, such an overestimate would not significantly affect the concentration fields calculated by the CALPUFF simulations, except for less than 2.1% of the time during short episodic rain events.

I-9.4 Exposure Concentrations at the SSFL Boundary

I-9.4.1 Frequency Distribution of Daily Average Concentrations for the Population with the Greatest Exposure

It is estimated that from 1975 to 1988, between 4 and 31 kerosene rocket fueled tests took place yearly. From 1977 to 1990, it is estimated that as little as 4 to 25 hydrazine (and derivatives) rocket fueled tests took place yearly. This means that the number of kerosene and hydrazine rocket tests in these years was or may have been less than 10% of the number of days in a year. Under such limited rocket engine testing, the calculated four-year hourly averages represent the most likely yearly concentrations in populated areas from these rocket tests. However, this best estimate does not indicate the extent of potential population exposure to significantly lower or higher concentrations in a single year with between 4 and 31 tests. The above concentration limits can be assessed by analysis of the four-year concentration frequency distribution.

The daily average concentration cumulative frequency distribution, for the population exposed to the greatest concentrations (at the SSFL property boundary), is shown in **Fig. I-10**. The arithmetic daily mean concentration of 1.36 $\mu g/m^3$ for a 1 g/s emission rate was taken as the baseline estimate. As shown in Fig. I-10, the concentration on 50% of the days are below the mean value of 1.36 $\mu g/m^3$ and 50% of the days are above. The daily minimum concentration of 0 $\mu g/m^3$ (no impact) occurred (on the average) during 19 days a year. The daily maximum concentration is 7.47 $\mu g/m^3$ and the daily concentration standard deviation is 1 $\mu g/m^3$.

The daily concentrations distribution is shown in **Fig. I-11**. A concentration of 0.25 $\mu g/m^3$ equals the mean log normal value of -1.39. The mean log normal concentration of 0.25 $\mu g/m^3$ is about 5 times less than the arithmetic mean concentration of 1.36 $\mu g/m^3$ designated as the baseline estimate. The log concentration distribution is skewed with 20% of the log concentrations below the mean and 80% greater than the mean.

Figure I-10. Daily average concentration frequency distribution for the population with the greatest exposure. Rocket engine test simulation is of increase testing from 6 a.m. to 7 p.m.

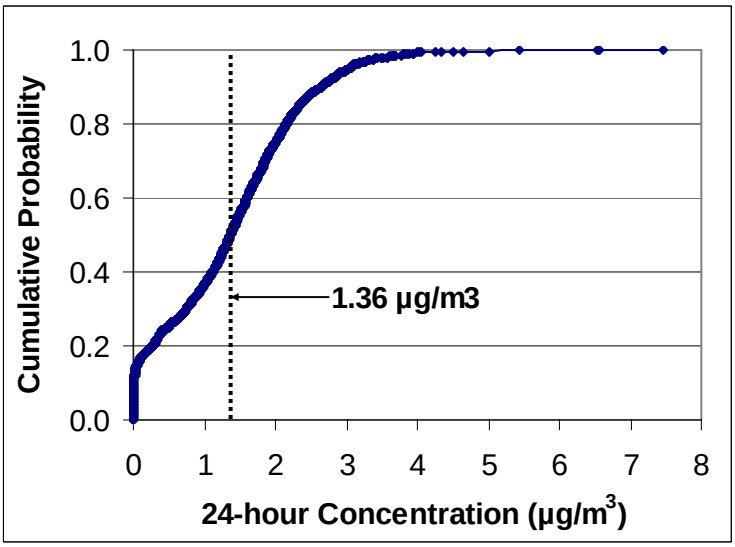

Figure I-11. Log concentration daily frequency distribution from four-years of meteorological data for the population with the greatest exposure.

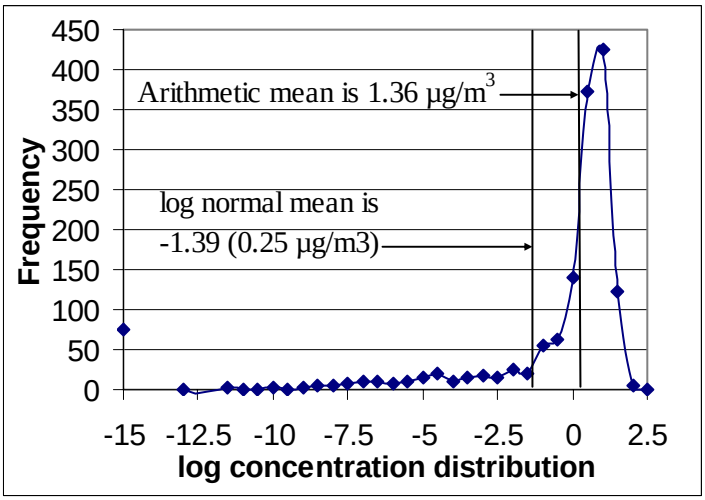

Averaging of the four lowest and four highest 24-hour average concentrations from the four years simulated reveals the following. The four lowest concentrations are all zero (no impact). The average of the four highest 24-hour concentrations is 6.5 µg/m^3. These averages mean that in any single year the population exposed to the greatest hourly average concentration may have been exposed from four tests to a concentration as low as zero and as high as 6.5 µg/m^3 compared with the arithmetic mean concentration of 1.36 µg/m^3 (i.e., the baseline estimate).

I-9.4.2 Diurnal Concentration Profile for the Population with the Greatest Exposure

For the population exposed to the greatest hourly average concentration (at the SSFL property boundary), the hourly average concentration increases during the day from 6 a.m. to 7 p.m. (Fig. I-12). The hourly average peak concentration is 7.82 µg/m^3 and occurs from 6 p.m. to 7 p.m. As shown in Fig. I-13, the peak hourly maximum concentration is during 4 p.m. to 5 p.m. (i.e., late afternoon).

Figure I-12. Diurnal profile of hourly average concentration at the SSFL property boundary. Rocket engine test simulation is of increase testing from 6 a.m. to 7 p.m.

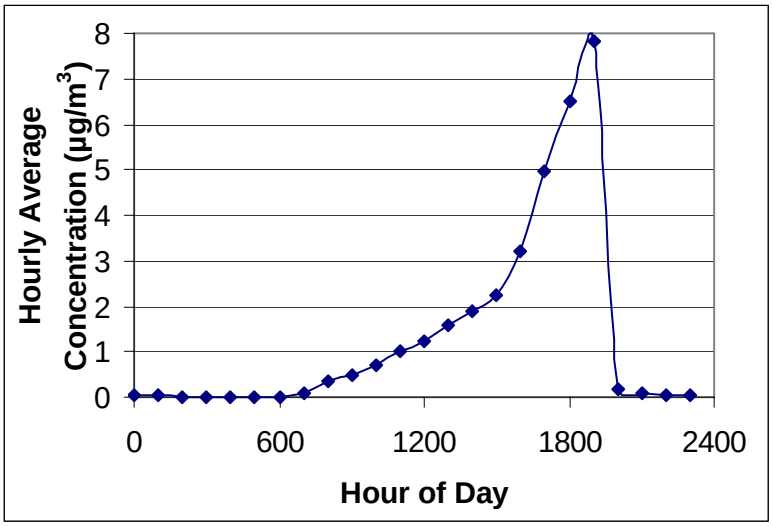

Figure I-13. Diurnal profile of hourly maximum concentration at the SSFL property boundary. Rocket engine test simulation is of increase testing from 6 a.m. to 7 p.m.

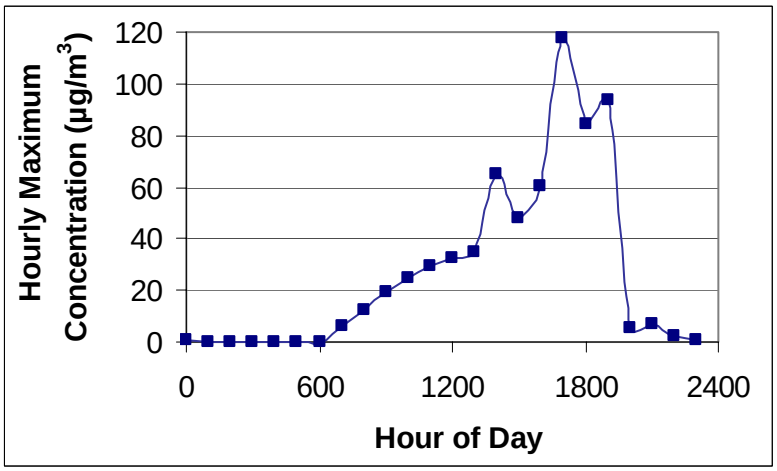

I-9.4.4 Worst Case Impact from a Single Rocket Engine Test

Analysis of a single emission event during the day with the highest emission was undertaken to assess the impact of a single rocket engine test testing during the period of 6 p.m. to 7 p.m. A shown in **Fig. I-14**., the resulting concentrations (for an emission rate of 1 g/s) decline away from SSFL (downwind distance) reveals a concentration decline by a factor of ten over a distance of less than five kilometers (3 miles).

Figure 0-1. Worst impact from a single rocket engine test. Hourly maximum concentration as a function of downwind distance. Downwind distance starts from the highest impacted populated area.

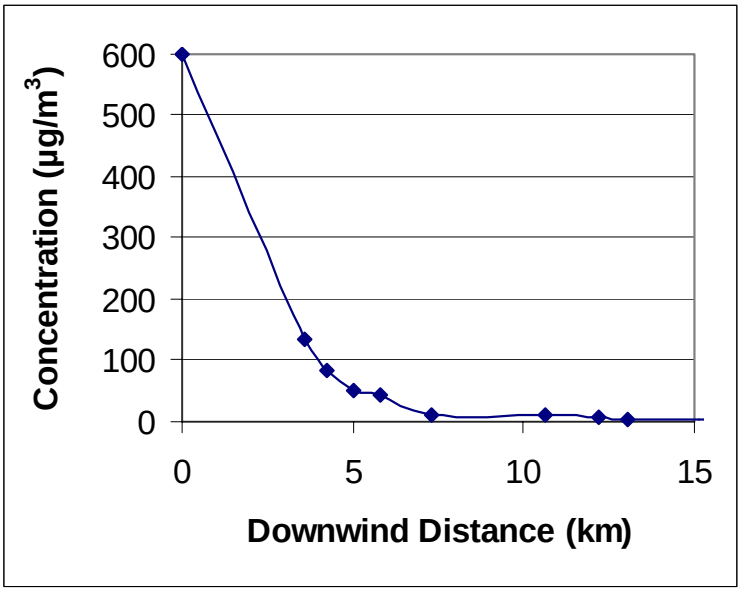

I-9.4 Summary of Sensitivity Analysis

A relative ranking of the potential importance of alternative air dispersion modeling treatments compared with the baseline estimate of airborne concentrations is summarized in Table I-6. For the baseline estimate emission scenario, the hourly maximum concentration is 100 times the hourly average concentration. The four-year daily concentration distribution identifies the possible daily average on years with four tests as being 5 times greater or 1000 times less compared with the baseline estimate of hourly averages. Neither atmospheric degradation chemistry, dry deposition nor wet deposition are likely to significantly reduce near-field concentrations. For example, atmospheric degradation reduces hydrazine concentrations by 1 to 3% in the near field, a factor of two on average, and in least impacted areas by a factor of ten. Dry deposition of particulates reduces concentrations by 0.5% to 0.8% in the near field, 15%-30% on average, and in least impacted areas by a factor of two. Wet deposition is expected to reduce annual averaged concentrations by no more than about 2.1%.

The results of the sensitivity studies should prove useful in guiding refinement of expanded sensitivity studies and future modeling efforts. It is important to note that, in order to refine the sensitivity analysis, there is need for accurate information regarding the number and timing of rocket tests and the meteorology associated with those tests. Unfortunately, the meteorology associated with individual tests may be difficult to reconstruct lacking routine nearby meteorological measurements from the start of testing (1948) to present (2004).

Table I-6. Ranking the Importance of Alternative Simulation Scenarios

Alternative Simulation Scenarios	Concentration Decrease (except as noted)
Hourly Maximum compared with Hourly Average	
Maximum Impact in Populated Area	Increase by factor of 100
Average Impact in Populated Areas	Increase by factor of 100
Minimum Impact in Populated Areas	Increase by factor of 100
Frequency Distribution	Potential decrease from 1.36 to 0
effect of Meteorology	$\mu g/m^3$; potential increase by factor of 5
Chemistry[(a)] – Hydrazine and 1,3-Butadiene	
Maximum Impact in Populated Area	1%-3%
Average Impact in Populated Areas	Factor of 2
Minimum Impact in Populated Areas	Factor of 2-10
Dry Deposition – Particulates	
Maximum Impact in Populated Area	0.5%-0.8%
Average Impact in Populated Areas	15%-30%
Minimum Impact in Populated Areas	Factor of 1.7-2.1
Wet Deposition	2.1%

[(a)] – atmospheric degradation